Predicting Forbidden and Allowed Cycloaddition Reactions: Potential Surface Topology and Its Rationalization

FERNANDO BERNARDI,*[1a] MASSIMO OLIVUCCI,[1b] and MICHAEL A. ROBB*[1b]

Dipartimento di Chimica "G. Ciamician" dell'Università di Bologna, Via Selmi 2, 40126 Bologna, Italy, and the Department of Chemistry, King's College London, Strand, London WC2R 2LS, U.K.

Received April 25, 1990 (Revised Manuscript Received August 6, 1990)

The objective of this Account is to discuss the theoretical information that is available on the mechanisms of forbidden and allowed cycloaddition reactions from a unified point of view.

We believe that theoretical investigations of chemical reactivity ought to have two facets. Firstly one must be concerned with the *numerical computation*[2,3] of the equilibrium structures, transition structures, reaction paths, and barriers that are associated with various competing mechanisms. Secondly, one must attempt to rationalize the results for a spectrum of related reactions with a model that gives us some *understanding* and permits easy visualization of the results. We have now completed numerical ab initio studies for several different cycloaddition reactions[4-9] and demonstrated[10] that they can all be understood (both qualitatively and quantitatively) in terms of the same simple valence-bond (VB) model.[11] Recently, in an application to the mechanism of the Cope rearrangement,[12] we have shown how a simple qualitative summary of very detailed ab initio results can be obtained by parametrizing this VB model and visualizing the results as 3D contour diagrams in selected important geometrical parameters. Here, we shall use this technique to give a unified discussion of the mechanisms of cycloaddition reactions.

Ground- and Excited-State 2 + 2 Cycloadditions

Potential Surface Topology. It is appropriate to start our discussion with the Woodward–Hoffmann[13] (ground state) forbidden and (excited state) allowed pathways for the 2 + 2 cycloaddition of two ethylene molecules in order to establish a reference point and to introduce the VB model[11] that can be used to rationalize the results. This reaction involves four active orbitals (i.e., involved in bond breaking or making) shown in Scheme I. After orbital mixing, since the HOMO of the reactants correlates with an excited orbital of the product, the electronic configuration changes between reactants and products and the reaction is said to be forbidden. The resulting avoided crossing is predicted to create a barrier on the ground-state potential surface (S_0) and a minimum on the doubly excited state surface

Scheme I

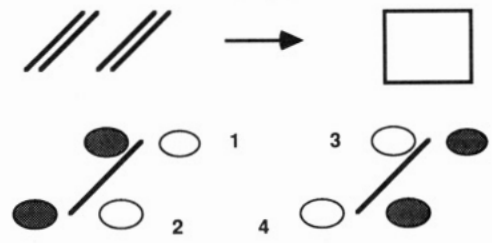

(S_2). On the other hand, the singly excited state S_1 correlates directly with the S_1 state of the products so that the excited-state reaction is said to be allowed. (The notation S_1 and S_2 is intended to indicate the lowest energy singly excited and doubly excited states, respectively). It is usually supposed[14,15] that the photochemical cycloaddition proceeds from an exciplex minimum on S_1 via a barrier associated with a crossing from S_1 to S_2 so that the excited-state cycloaddition ultimately pauses[15] in the S_2 minimum before radiationless decay to the ground state takes place. Thus the radiationless decay from S_2 to S_0 is assumed[14,15] to be very fast and occurs after the rate-determinine step. However, consideration of the dynamics of systems passing through the pericyclic minimum (see, for example, ref 17a, pp 153–156) shows that if the S_0–S_2 gap

Fernando Bernardi received his degree in industrial chemistry at the University of Bologna (Italy) in 1962 and did postgraduate work at the University of Cambridge (1969–1971). His present position is full Professor of Advanced Organic Chemistry at the Dipartimento di Chimica G. Ciamician of the University of Bologna. His research interests span all aspects of theoretical organic chemistry.

Massimo Olivucci studied at the University of Bologna, obtaining the Laurea in Chimica in 1984 and the Ph.D. in 1989. He is currently employed as a postdoctoral research assistant at King's College London.

Michael Robb obtained B.Sc. (1966) and Ph.D. (1970) degrees at the University of Toronto and the D.Sc. at London University in 1988. His current post is Reader in Chemistry at King's College London. In addition to applications in organic chemistry, he has interests in the development of methodology in MC-SCF, effective Hamiltonian methods, and unitary groups.

(1) (a) Dipartimento di Chimica "G. Ciamician" dell'Università di Bologna. (b) Chemistry Department, Kings's College London.
(2) Ab initio methods in Quantum Chemistry I. Lawley, H. P., Ed. *Adv. Chem. Phys.* **1987**, *67*.
(3) Ab initio methods in Quantum Chemistry II. Lawley, K. P. Ed. *Adv. Chem. Phys.* **1987**, *69*.
(4) Bernardi, F.; Bottoni, A.; Robb, M. A.; Schlegel, H. B.; Tonachini, G. *J. Chem. Soc.* **1985**, *107*, 2260–2264.
(5) Bernardi, F.; De, S.; Olivucci, M.; Robb, M. A. *J. Am. Chem. Soc.* **1990**, *112*, 1737–1743.
(6) Bernardi, F.; Bottoni, A.; Field, M. J.; Guest, M. F.; Hillier, I. H.; Robb, M. A.; Venturini, A. *J. Am. Chem. Soc.* **1988**, *110*, 3050–3055.
(7) McDouall, J. H. W.; Robb, M. A.; Niazi, V.; Bernardi, F.; Schlegel, H. B. *J. Am. Chem. Soc.* **1987**, *109*, 4642.
(8) Tonachini, G.; Schlegel, H. B.; Bernardi, F.; Robb, M. A. *J. Am. Chem. Soc.* **1990**, *112*, 483–490.
(9) Bernardi, F., Bottoni, A.; Robb, M. A., Venturini, A. *J. Am. Chem. Soc.* **1990**, *112*, 2106–2114.
(10) Bernardi, F.; Olivucci, M.; Robb, M. A. *Res. Chem. Intermed.* **1989**, 217–249.
(11) (a) Bernardi, F.; Olivucci, M.; McDouall, J. J. W.; Robb, M. A. *J. Chem. Phys.* **1988**, *89*, 6365. (b) Robb, M. A.; Bernardi, F. In *New Theoretical concepts for Understanding Organic reactions* (Bertran, J., Csizmadia, I. G., Eds.; Kluwer Acadmeic Publishers Hingham, MA), 1989; pp 101–146.
(12) Bearpark, M.; Bernardi, F.; Olivucci, M.; Robb, M. A. *J. Am. Chem. Soc.* **1990**, *112*, 1732–1736.
(13) Woodward, R. B.; Hoffmann, R. *Angew. Chem., Int. Ed. Engl.* **1969**, *8*, 781–853.
(14) (a) Turro, N. J. *Modern Molecular Photochemistry*; Benjamin Publishing: Reading, MA, 1978. (b) Michl, J.; Bonacic-Koutecky, V. *Electronic Aspects of Organic Photochemistry*; Wiley: New York, 1990.
(15) (a) Caldwell, R. A. *J. Am. Chem. Soc.* **1980**, *102*, 4004–4007. (b) Caldwell, R. A.; Creed, D. *Acc. Chem. Res.* **1980**, *13*, 45–50.
(16) Dewar, M. J. S. *J. Am. Chem. Soc.* **1984**, *106*, 209–219.

0001-4842/90/0123-0405$02.50/0

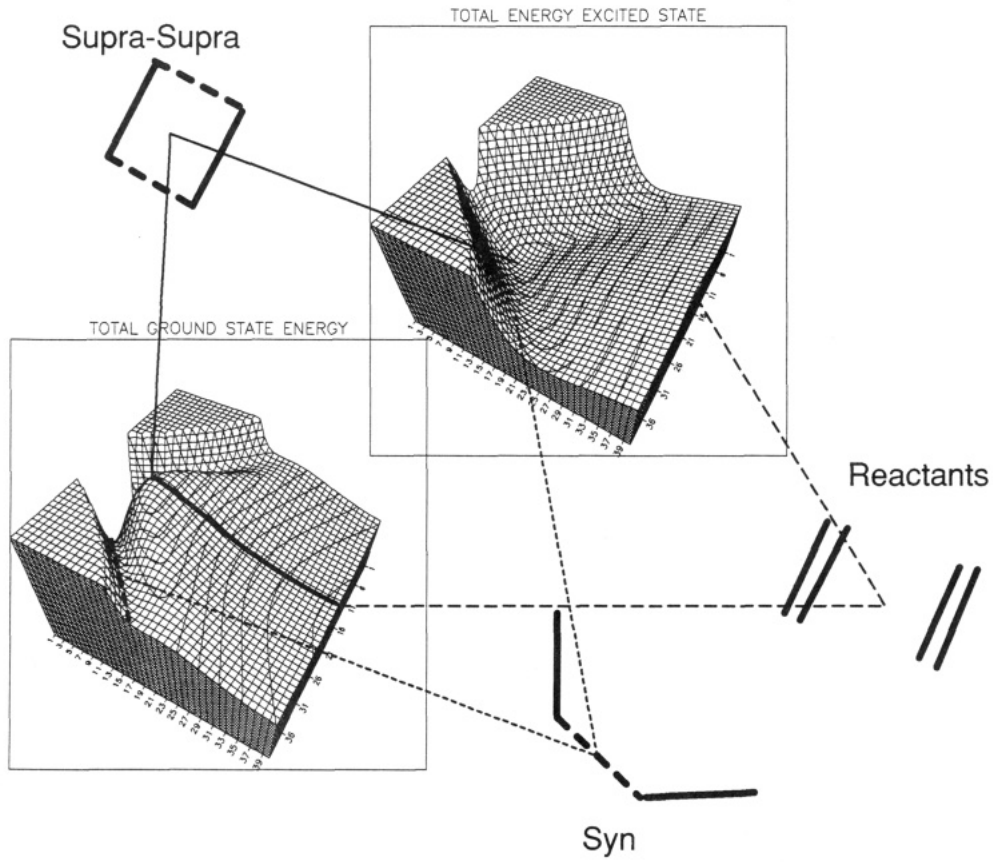

Figure 1. Potential energy surfaces (S_2 top, S_0 bottom) for the $2_s + 2_s$ cycloaddition of two ethylene molecules. The X axis (diagonal top left to bottom right) is the interfragment distance R, and the Y axis (diagonal top right to bottom left) is the angle α (C–C···C). The remaining geometrical parameters are interpolated between reactants, transition states, and products. Each division on the X axis corresponds to an increment of $0.1a_0$ (0.053 Å), and the first division corresponds to $R = 3.5\ a_0$ (1.85 Å). Each division on the Y axis correspond to an increment of 3.5°, and the first division corresponds to $\alpha = 20°$.

is greater than a few kilocalories/mole, then the decay rate is very small.

The term *forbidden*[13] when applied to the ground state is usually assumed to imply a very high barrier for the concerted path with a preference for a lower energy nonconcerted path. In contrast, for an *allowed* reaction, any barrier is expected to be dominated by steric factors. While it is usually proposed that allowed reactions are synchronous and concerted, the asynchronous paths may exist and one has a competition that has been the subject of some controversy.[16]

We have performed MC-SCF computations on the concerted and nonconcerted pathways[4] for this reaction in 1985, and our excited-state results have just been published.[5] It is useful to discuss these results using potential energy surface contour diagrams that have been designed to reproduce these ab initio data.[11,12] The ab initio results for S_0 and S_2 are summarized in Figure 1. The synchronous pathway is shown as a solid line on the ground-state surface while motion on the asynchronous pathway is shown as a dashed line on the ground-state surface. We see the expected behavior for a forbidden reaction: (1) the ground-state synchronous path has a local maximum (rather than a true transition state) so that the reaction must proceed via the lower energy asynchronous channel (containing a syn transition state[4]), and (2) the excited-state surface S_2 has a local minimum at approximately the same geometry as the antiaromatic local maximum on S_0.

However, this simple picture is naive and becomes modified when other possible motions are examined. We discuss the ground state first. The syn transition state on the asynchronous pathway turns out to be a local maximum when rotation about an interfragment C···C bond is examined. Thus the syn asynchronous path does not exist and there must exist lower energy pathways. In fact one finds[4] reaction paths for gauche and anti conformations. Further, all the asynchronous paths are unconcerted (i.e., there are an intermediate and two transition states on each path). As a consequence, there is a ridge that separates reactants and biradical intermediates with true transition state for gauche and anti conformations. The anti biradical minimum has a C–C bond length of 1.65 Å and lies only 0.38 kcal mol^{-1} below the fragmentation transition state. Thus our 4-31G MC-SCF computations[4] predict an asynchronous biradical pathway that is nonconcerted.

Now let us turn our attention to the excited-state reaction.[5] It is very difficult to obtain information about the state S_1 (singly excited state) since this will be a Rydberg state and the crossing S_1/S_2 (S_2 is doubly excited) will be associated with a Rydberg to valence transformation. From Figure 1, the S_2 surface appears to have a minimum at approximately the same geom-

(17) (a) Salem, L. *Electrons in Chemical Reactions: First Principles*; Wiley: New York, 1982. (b) Tully, J. C.; Preston, R. K. *J. Chem. Phys.* **1971**, *55*, 562. (c) Von Neumann, J.; Wigner, E. *Phys. Z.* **1929**, *30*, 467. (d) Teller, E. *J. Phys. Chem.* **1937**, *41*, 109. (e) Herzberg, G.; Longuet-Higgins, H. C. *Trans. Faraday Soc.* **1963**, *35*, 77. (f) Herzberg, G. *The Electronic Spectra of Polyatomic Molecules*; Van Nostrand: Princeton, NJ, 1966; pp 442. (g) Mead, C. A.; Truhlar, D. G. *J. Chem. Phys.* **1979**, *70*, 2284. (h) Mead, C. A. *Chem. Phys.* **1980**, *49*, 23. (i) Keating, S. P.; Mead, C. A. *J. Chem. Phys.* **1985**, *82*, 5102. (j) Keating, S. P.; Mead, C. A. *J. Chem. Phys.* **1987**, *86*, 2152.

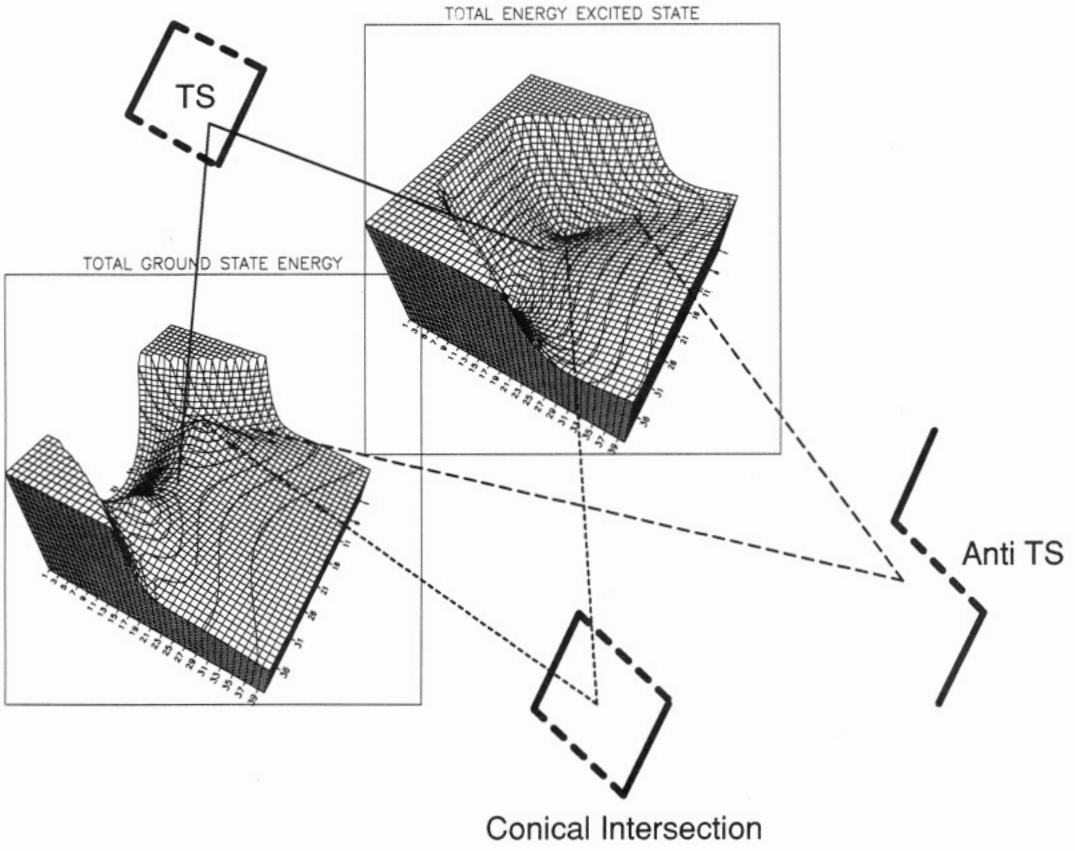

Figure 2. Potential energy surfaces for the ground-state S_0 (bottom left) and excited-state S_2 (top right) 2 + 2 cycloaddition of two ethylene molecules. The X axis (diagonal top left to bottom right) is the interfragment distance R, and the Y axis (diagonal top right to bottom left) is the angle τ (the coordinate that connects the antiaromatic with the anti structure, corresponding to C···X_1···X_2 where X_i is the midpoint of the C–C bond in the ethylenic fragment. Each division on the X axis corresponds to an increment of 0.1 a_0 (0.053 Å), and the first division corresponds to $R = 3.0a_0$ (1.58 Å). Each division on the Y axis corresponds to an increment of 3.5°, and the first division corresponds to $\alpha = 20°$. The values of the remaining geometrical parameters have been interpolated with respect to R.

etry as the "antiaromatic" transition state on the S_0 surface. The S_0–S_2 gap at this geometry is approximately 60 kcal mol^{-1} so the probability of radiationless decay from S_2 to S_0 will be very small. Again, this picture is too simple and changes when other possible nuclear motions are considered. Remarkably, the structure that corresponds to the "antiaromatic" geometry on the excited-state surface turns out to be a transition state that connects the two equivalent ground-state anti geometries. The ground- and excited-state surfaces are shown in Figure 2 in the space that corresponds to variables R and τ (which corresponds to the negative direction of curvature that connects the excited-state S_2 antiaromatic structure with the ground-state S_0 anti structure). It can be seen that we have a novel topological feature: a conical intersection.[17] The bottom part of the double cone lies on the ground-state surface between the $2_s + 2_s$ S_0 reaction path and the anti asynchronous "channels". The other half of the double cone lies on the excited-state surface. Chemically, once the reaction arrives on the S_2 surface, it is able to cross directly to the ground-state surface via the conical intersection. The existence of such topological features is an important feature in the mechanism since it permits a fully efficient return from S_2 to S_0. Thus one can now understand why the reaction rate is controlled[14,15] by the presence of minima and transition states on S_0 and S_1/S_2 themselves rather than rate of radiationless decay from S_2 to S_0 (which would be very small[17a] for a gap larger than a few kilocalories/mole).

To conclude this section, we should mention the allowed $2_s + 2_a$ reaction pathway. In fact the transition structure is a local maximum[18] with a negative direction of curvature along R and a second negative direction of curvature that leads to the syn gauche transition state. Thus the $2_s + 2_a$ path does not exist.

A Rationalization Using a Valence-Bond Model. Now let us turn our attention to attempting to understand the origin of the topological features of the potential surfaces. We shall look for insight by decomposing the total energy of the molecule into component parts have a simple interpretation. We shall carry out this decomposition in two complementary ways: (i) via a diabatic surface model[11,19] and (ii) via the total[11] coulomb (Q) and exchange energy (T). Both these methods are based upon a simple VB model that has the important feature that it can be implemented[11] to reproduce the energetics of the MC-SCF computations *exactly*.

Each of these energy decomposition methods yields complementary information. In the diabatic surface model, the origin of the reaction barrier is associated with a change of spin coupling from that of the reactant bonding diabatic state to that of the VB product bonding diabatic state. For our model system there are only two diabatic states that need to be considered (Scheme II). The resonance between the diabatics is

(18) Bernardi, F.; Bottoni, A.; Olivucci, M.; Robb, M. A.; Schlegel, H. B.; Tonachini, G. *J. Am. Chem. Soc.* **1988**, *110*, 5993–5995.
(19) (a) Evans, G.; Polanyi, M. *Trans. Faraday Soc.* **1938**, *34*, 11. (b) Evans, G.; Warhurst, E. *Trans. Faraday Soc.* **1938**, *34*, 614.

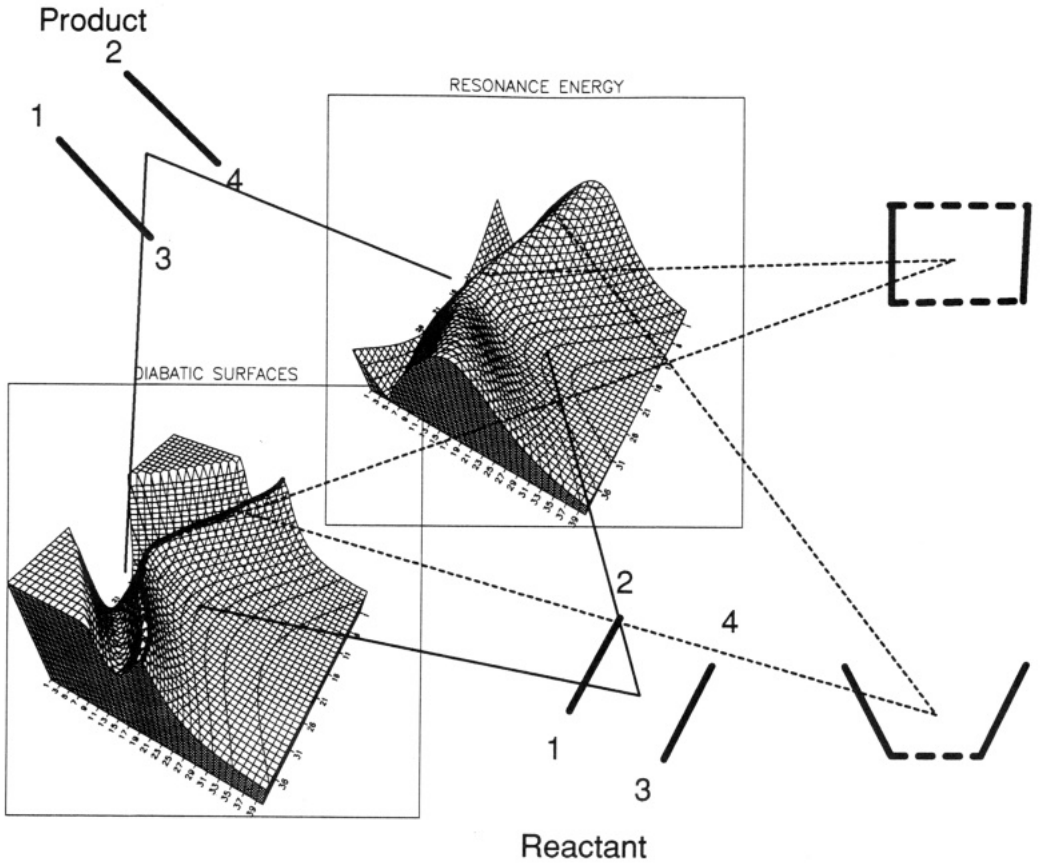

Figure 3. Diabatic potential energy surfaces (eq 1, lowest energy sheet) and resonance energy surfaces (β as defined in eq 2) for the $2_s + 2_s$ cycloaddition of two ethylene molecules. The X and Y axes are defined as in Figure 1.

Scheme II

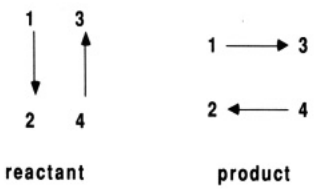

familiar as a theoretical measure of aromaticity. This type of model may be familiar to the reader from the work of Shaik,[20] where it has been applied in an empirical way to S_N2 reactions. In contrast, the decomposition[11] of the total energy into the quasi-classical coulomb energy Q and into the total exchange energy $-T$ is more directly related to concepts from structural organic chemistry. The quasi-classical coulomb energy Q depends mainly upon the nonbonded repulsions and steric effects. Thus the term Q can be thought of as the energy of the system if all the bonding interactions between the reactive sites are "switched off". In constrast, $-T$ is a direct measure of the bonding energy effects for the *active* electrons (i.e., those involved in bond making and breaking). The VB Hamiltonian[11] is a function of coulomb integrals (Q_{ij}) and exchange integrals (K_{ij}) that depend on the distance between the sites of the "active" (i.e., involved in bond making and breaking) atomic orbitals i and j. For the purposes of qualitative interpretation, these integrals can be assumed to have the same form as the Heitler–London VB treatment of H_2.

(20) (a) Pross, A.; Shaik, S. S. *Acc. Chem. Res.* **1938**, *16*, 363. (b) Shaik, S. S. *Prog. Phys. Org. Chem.* **1985**, *15*, 198–337.

We begin with a discussion of the diabatic surface decomposition. In Figure 3 we show behavior of the diabatic surfaces α_R/α_P and the resonance energy β for the (α,R) space used in Figure 1 for the ground- and excited-state total energies. The energy of the reactant and product diabatic states for any geometry is given as[11]

$$\alpha_R = Q + K^* \tag{1a}$$

$$\alpha_P = Q - K^* \tag{1b}$$

The quantity α_R is the energy of the reactant bonding configuration (Scheme II), and α_P is the energy of the product bonding configuration. We shall refer to K^* as the "bond exchange energy". It is a function of the difference in the exchange energy of the reactant and product VB structures. The most important observations are that (i) the reactant diabatic α_R is repulsive and the product diabatic α_P is attractive and (ii) the diabatic surfaces α_R/α_P intersect in a ridge (with $K^* = 0$) in the transition-structure region.

The total energy is given as

$$E = \frac{1}{2}\{\alpha_R + \alpha_P \pm [(\alpha_R - \alpha_P)^2 + 4\beta^2]^{1/2}\} \tag{2}$$

or

$$E = Q \pm [(K^*)^2 + \beta^2]^{1/2} \tag{3}$$

The quantity β is the resonance energy. From Figure 3 one can see that the topology of ground- and excited-state surfaces is controlled by the resonance energy β. Since β is smaller in the region of the antiaromatic transition structure than in the region of the syn reaction pathway, we obtain a local maximum on the

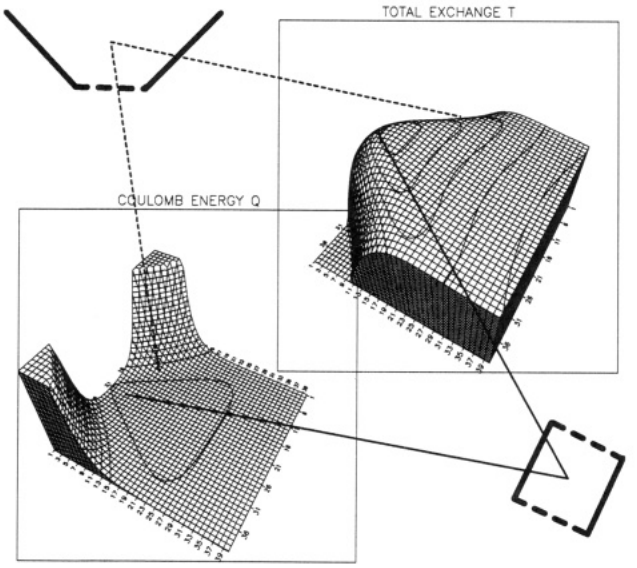

Figure 4. Coulomb potential energy surfaces (Q) and exchange energy surfaces ($-T$ as defined in eq 4) for the $2_s + 2_s$ cycloaddition of two ethylene molecules. The X and Y axes are defined as in Figure 1.

ground-state surface and a local minimum on the excited surface.

Now let us examine a different partition of the total energy into coulomb (Q) and total exchange ($-T$) contributions. This decomposition in the R,α space is shown in Figure 4. We define the total exchange energy as

$$T = [(K^*)^2 + \beta^2]^{1/2} \tag{4}$$

and thus

$$E = Q \pm T \tag{5}$$

From Figure 4 there are two important observations: (i) Q is almost completely flat, and (ii) $-T$ has a pronounced local maximum and becomes attractive more rapidly along an asynchronous coordinate. Because of feature i, the topology of the total energy surface is completely controlled by $-T$. On the reactant side of the ridge separating reactants and products, we are breaking π bonds so that the $-T$ (Figure 4) surface is weakly repulsive, and on the product side, we are forming new σ bonds so that the $-T$ surface is very strongly attractive.

The power of the VB model is that it permits a simple rationalization of the topology of the S_2 surface (the conical intersection) as well as the ground-state surface. (The present discussion should be compared with the two-orbital two-electron model[21] for conical intersections proposed by Michl and his co-workers for biradicaloid structures.) It is convenient to define K_P as the exchange energy of the products ($K_{13} + K_{24}$), K_R as the exchange energy of the reactants ($K_{12} + K_{34}$), and K_X as the nonbonded exchange energy ($K_{14} + K_{23}$). At a conical intersection, where the energies of the ground and excited states are equal (i.e., $T = 0$), two alternative conditions exist: (i) a condition on α_R, α_P, and β (via eq 2a),

$$\alpha_R = \alpha_P \ (K^* = 0) \text{ and } \beta = 0 \tag{6}$$

or alternatively,

(21) Bonacic-Koutecky, V.; Koutecky, J.; Michl, J. *Agnew. Chem., Int. Ed. Engl.* **1987**, *26*, 170–189.

$$T = [(K_P - K_X)(K_R - K_X) + (K_P - K_R)^2]^{1/2} \tag{7}$$

which gives (ii) a condition on T,

$$K_P = K_X, \ K_R = K_X, \text{ and } K_P = K_R \tag{8}$$

The behavior of these two (eqs 6 and 8) equivalent conditions is illustrated in Figure 5 in the space of R and τ (Figure 2). In the top half of the figure, one can observe the singularity corresponding to $T = 0$ (eq 8). In the lower half we have the condition of eq 6, $\alpha_R = \alpha_P$ (indicated by the solid line) on the left-hand side and $\beta = 0$ (trough indicated by solid line) on the right. The conical intersection corresponds to the situation where both conditions (eq 6) are simultaneously satisfied.

Two Allowed Cycloaddition Reactions: Diels–Alder and 1,3 Dipolar Cycloadditions

Let us begin our discussion with a brief review of the structural/energetic results that come from ab initio calculations.[6,7] For the Diels–Alder reactions,[6] there is now agreement that the C_s synchronous concerted transition structure is the lowest energy transition state. Our[6] MC-SCF calculations predict it to lie only 2.2 kcal mols^{-1} below the syn–gauche at the 4-31G level. Indeed, the biradicaloid region of the surface is very flat indeed like the corresponding region of the ethylene + ethylene surface. Similarly, MC-SCF computations at the 4-31G level predict[7] that 1,3 dipolar cycloadditions are also synchronous and concerted. Multireference CI gives a 13.4 kcal mol^{-1} preference for the concerted pathway for the cycloaddition of fulminic acid (HCNO) to acetylene.

Now let us turn to the more interesting question: What is the origin of this preference for a synchronous pathway? For allowed reactions the Woodward–Hoffmann scheme[13] makes the prediction that the reaction will most likely be concerted and synchronous with a low barrier controlled by steric/electrostatic effects rather than electronic rearrangement. In terms of the VB model used above, this would imply that the mechanistic preference turns out to be controlled by Q rather than $-T$. In fact, the picture turns out to be quite close to this naive view but for very subtle reasons.

In Figures 6 and 7 we give the total ground-state energy, diabatic surfaces, and resonance energy in the R,α space for comparison with the ethylene cycloaddition (Figure 1). (Since the central double bond in the butadiene fragment is passive in the region of the transition state and in the cycloaddition of fulminic acid (HCNO) to acetylene, the N lone pair behaves similarly, it is possible to use the same two resonance structures.) Notice that the total energy surfaces now have a proper *col* (i.e., transition state) rather than a local maximum. However, the *ridge is very flat*. The diabatic surface intersections are very similar to ethylene (Figure 3) indicating a similar origin to the reaction barrier (a change in spin-coupling). However, in contrast to the ethylene cycloaddition, the resonance energy has a slight maximum for the synchronous path yielding the mechanistic preference.

It is the decomposition into Q/T shown in Figures 8 and 9 that provides the insight into the difference between allowed and forbidden cycloaddition reactions. The most important observations are as follows:

(i) The surface of $-T$ (the total exchange energy) has a similar form in all three reactions and is characterized by the presence of a local maximum in the region of the

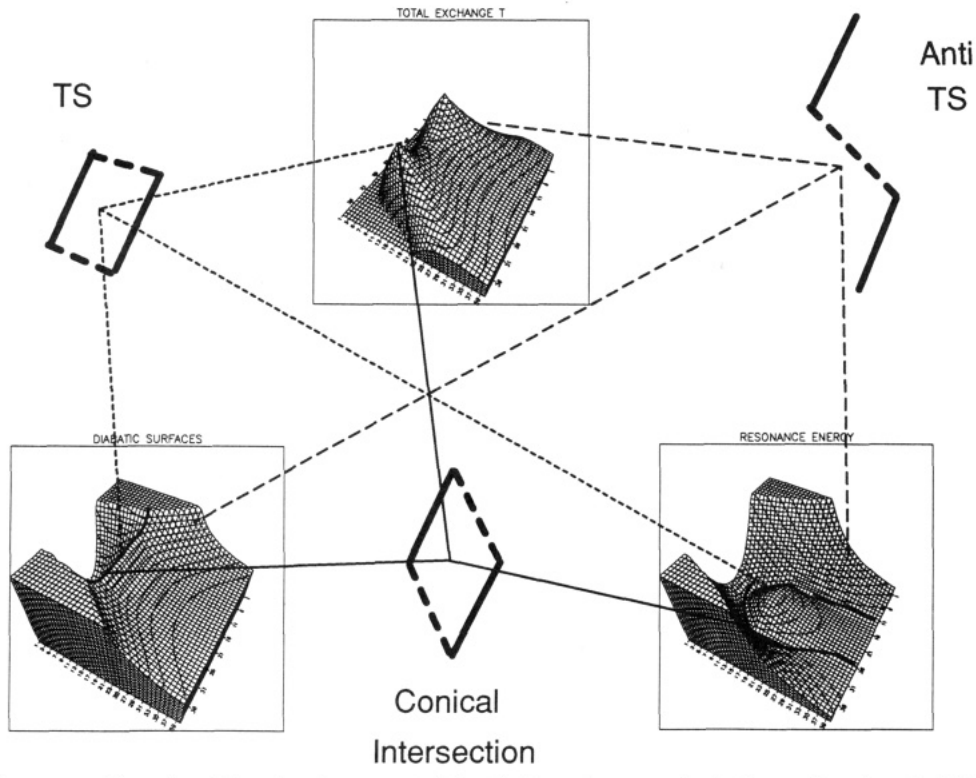

Figure 5. Potential energy surfaces for $-T$ (eq 4 or 7, top center) for the lowest energy sheet of α_R and α_P (eqs 1a, b, lower left), and for $|\beta|$ (eq 2), the resonance energy, in the space R,τ (Figure 2) for the 2 + 2 cycloaddition of two ethylene molecules. The X and Y axes are defined as in Figure 2. The ridge in the representation of α_R and α_P corresponds to the locus of points that satisfies the first condition of eq 6. The valley of $|\beta|$ corresponds to the second condition of eq 6, and the intersection of the ridge of α_R and α_P and the valley of $|\beta|$ corresponds for the geometry of the double cone in Figure 2.

supra–supra critical point (synchronous *transition* structure). Note that the curvature of $-T$ with respect to the direction α, evaluated at a point (R, $\alpha = 0$) for a concerted reaction path, depends critically upon the value of R: at large R (e.g., T in the Diels–Alder reaction, Figure 8), the curvature is positive, but as one approaches the critical point in $-T$ (i.e., small R), the curvature becomes negative (.e.g, $-T$ in the 1,3 dipolar cycloaddition reaction, Figure 9). Furthermore, in the transition-state region, the surface of $-T$ always favors the asynchronous pathway. The similarity of $-T$ is not too surprising since it is controlled mainly by the distances between the atomic sites involved in bond breaking and making.

(ii) In contrast, the surface for Q is very different in the three reactions. While this surface is almost completely flat in the ethylene + ethylene cycloaddition, it has pronounced minima for the Diels–Alder and 1,3 dipolar cycloadditions.

Thus, while in the ethylene + ethylene cylcoaddition the surface topology is controlled by $-T$, in the Diels–Alder and 1,3 dipolar cycloadditions the surface topology is controlled by a delicate balance between Q and $-T$.

Conclusions

In this Account we have given a discussion of theoretical results of forbidden and allowed cycloaddition that is unified by a common VB model.

This VB model indicates that the origin of the ridge that separates reactants and products is a change of spin coupling from that of the reactant bonding VB configuration to that of the product VB bonding configuration. This observation is a particular feature of the VB method and was first pointed out by Oosterhoff and co-workers[22] in their discussions of Woodward–Hoffmann rules using VB theory. The resonance energy can be taken as a theoretical measure of aromaticity. If one compares the resonance energy for the forbidden reaction in Figure 3 with the corresponding data for the two allowed reactions in Figures 6 and 7, one can see that the resonance energy has a maximum value at the transition state for the latter but is a minimum for the former (i.e. the allowed transition structure is more aromatic).

One the other hand, the behavior of the quasi-classical coulomb energy Q and the total exchange energy $-T$ is more directly related to concepts from structural organic chemistry. The quasi-classical coulomb energy Q depends mainly upon the nonbonded repulsions and steric effects while $-T$ is a direct measure of the bonding effects for the active electrons. The topology of the net bonding energy as manifested in $-T$ is the same for allowed and forbidden reactions, and it is the delicate balance of coulomb (Q) and exchange ($-T$) that is responsible for the preference for a synchronous pathway in the allowed reactions we have studied. This delicate balance can be easily upset by substituent effects for allowed reactions so that a broad spectrum of mechanisms must be expected. In contrast, for forbidden reactions, the behavior of the total exchange ($-T$) appears to dominate.

Finally, let us mention that these ideas can be easily applied in a qualitative way. The results of two other related cycloaddition reactions that we have recently

(22) van der Hart, W. J.; Mulder, J. J. C.; Oosterhof, L. J. *J. Am. Chem. Soc.* **1972**, *94*, 5724.

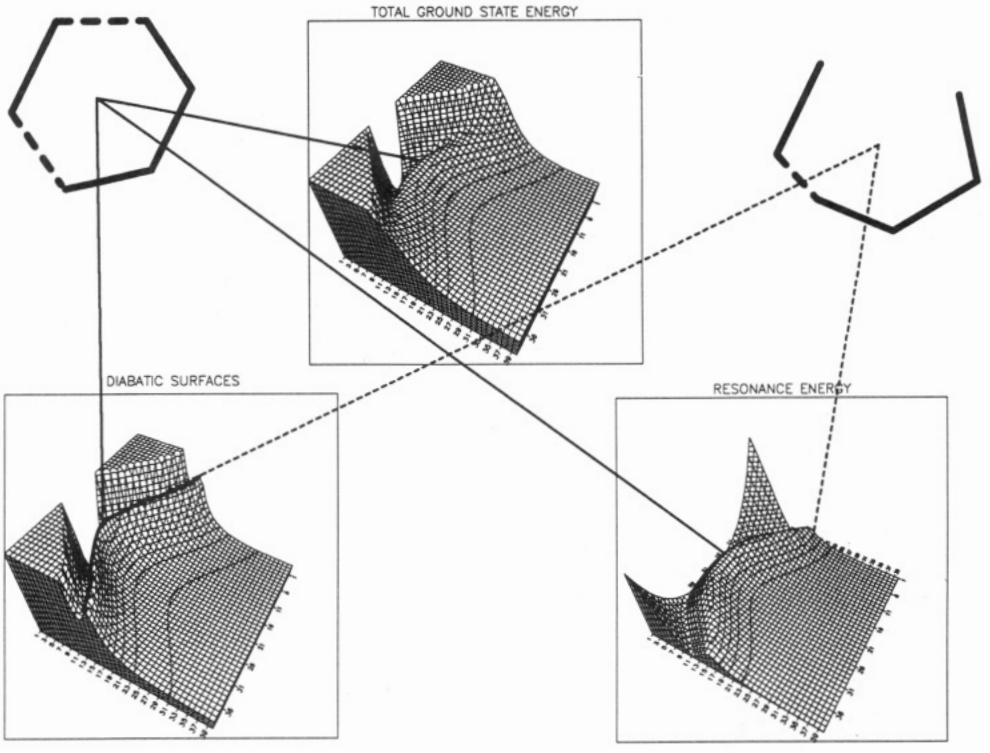

Figure 6. Potential energy surfaces for total energy (top center), for the lowest energy sheet of α_R and α_P (lower left), and for $|\beta|$, the resonance energy (lower right) for the Diels–Alder reaction of *cis*-butadiene and ethylene molecules. The X and Y axes are defined as in Figure 1. Each division on the X axis corresponds to an increment of 0.2 a_0 (0.105 Å), and the first division corresponds to R = 3.0 a_0 (1.58 Å). Each division on the Y axis corresponds to an increment of 3.5°, and the first division corresponds to α = 20°.

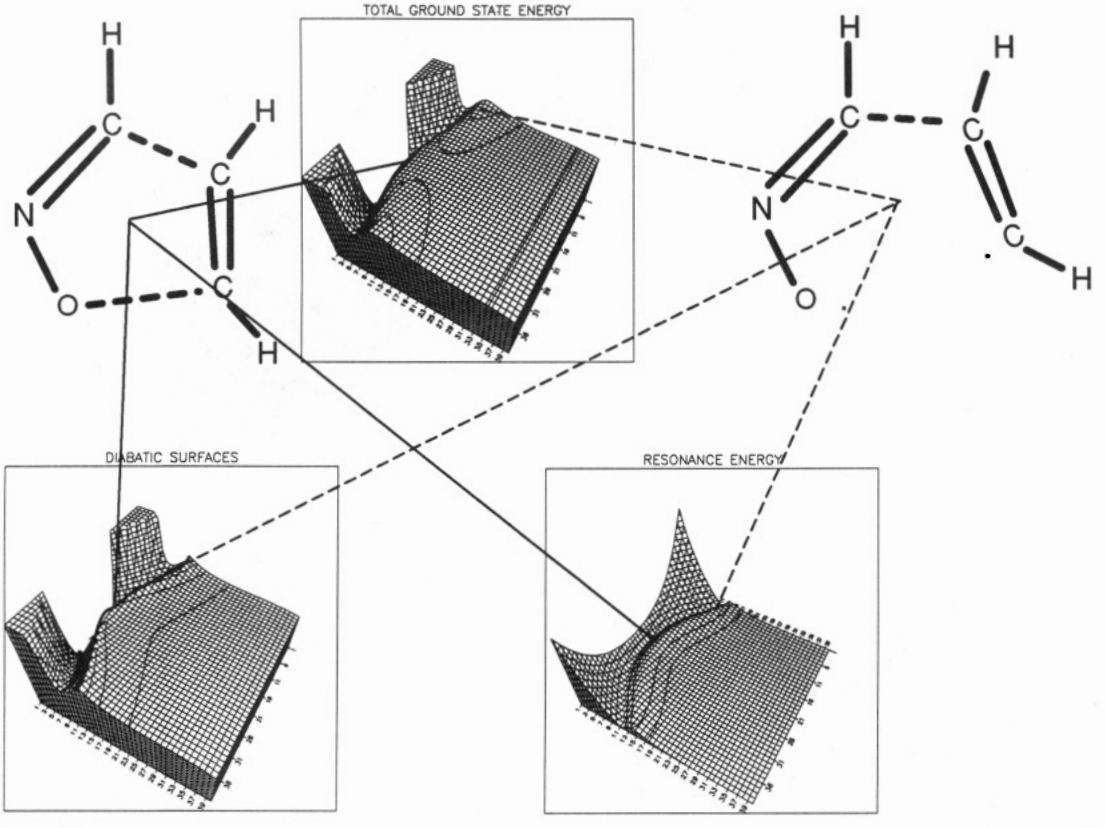

Figure 7. Potential energy surfaces for total energy (top center), for the lowest energy sheet of α_R and α_P (lower left), and for $|\beta|$, the resonance energy (lower right) for the 1,3 dipolar cycloaddition of fulminic acid (HCNO) and acetylene molecules. The X and Y axes are defined as in Figure 1. Each division on the X axis corresponds to an increment of $0.2a_0$ (0.105 Å), and the first division corresponds to R = $3.0a_0$ (1.58 Å). Each division on the Y axis corresponds to an increment of 3.5°, and the first division corresponds to α = 20°.

studied (cycloaddition of $^1\Delta_g$ O_2 with ethylene and ketene with ethylene[8,9]) are predictable from the simple VB model we have outlined earlier. Both reactions are complicated by the fact that ethylene can attack the π

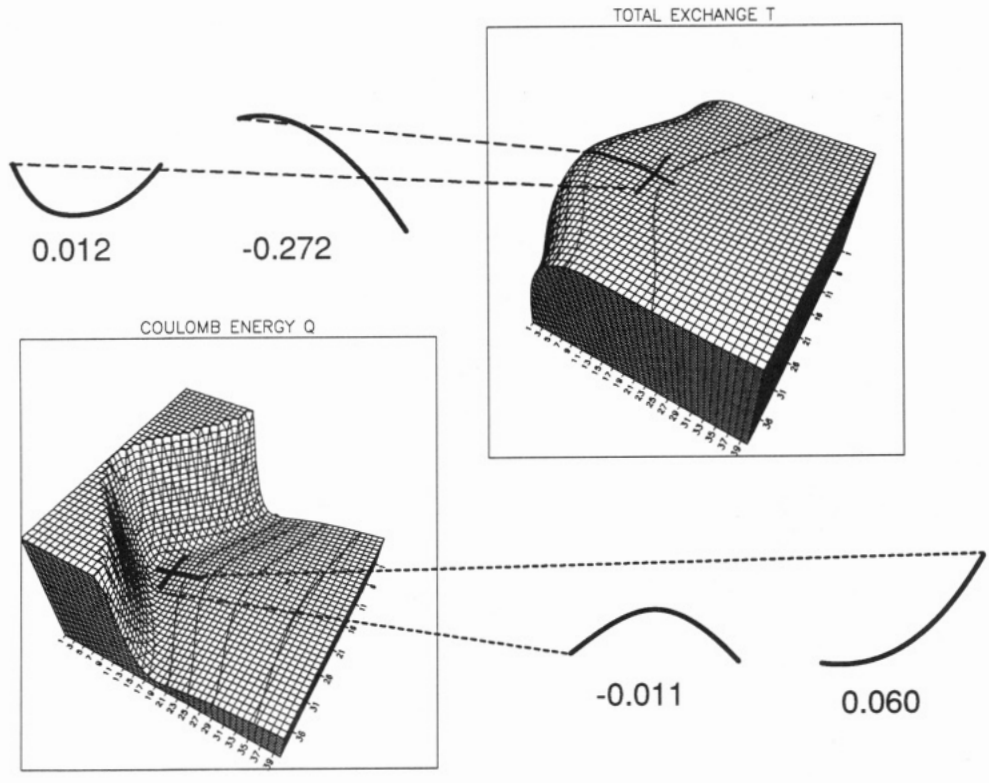

Figure 8. Potential energy surfaces, coulomb Q (bottom left) and exchange energy $-T$ (top right) for the Diels–Alder reaction of *cis*-butadiene and ethylene molecules. The X and Y axes are defined as in Figure 6. The position of the transition structure is indicated by a cross, and a sketch of a cross section along R and α is also indicated. The value of curvature ($\partial^2 Q/\partial q_i^2$ and $-\partial^2 T/\partial q_i^2$) for $q_i = \alpha$ and R is given beside each sketch.

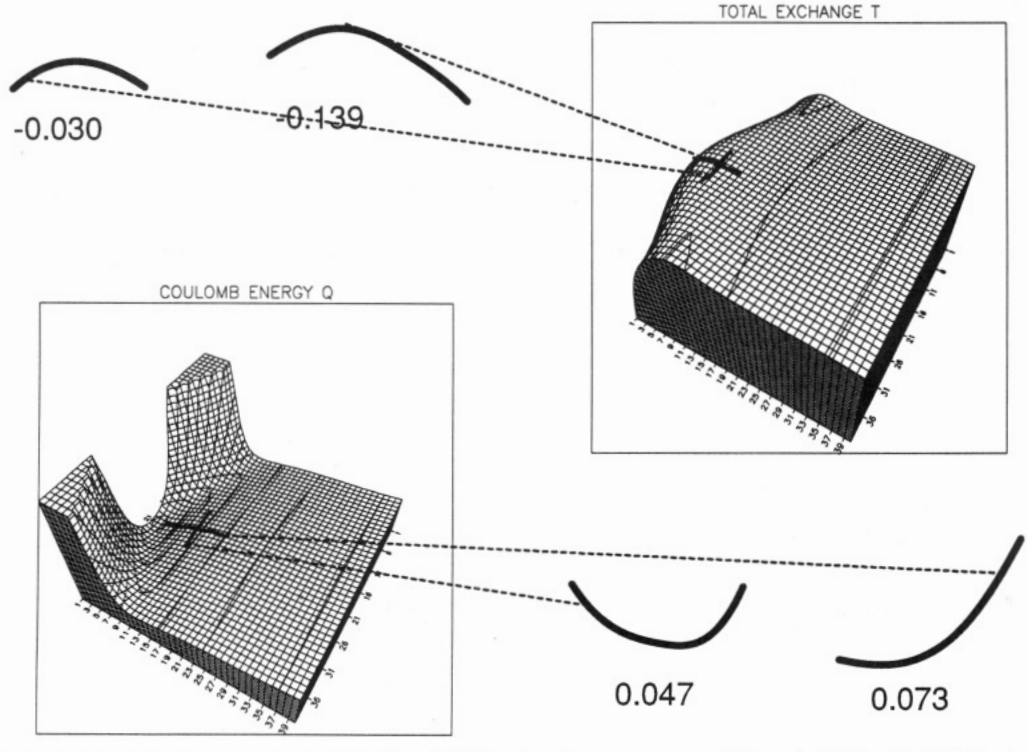

Figure 9. Potential energy surfaces, coulomb Q (bottom left) and exchange energy $-T$ (top right) for the 1,3 dipolar cycloaddition of fulminic acid (HCNO) and acetylene molecules. The X and Y axes are defined as in Figure 7. The position of the transition structure is indicated by a cross, and a sketch of a cross section along R and α is also indicated. The value of curvature ($\partial^2 Q/\partial_i^2$ and $-\partial^2 T/\partial q_i^2$) for $q_i = \alpha$ and R is given beside each sketch.

systems of O_2 and ketene in several ways, leading in both cases to two different products, one the analogue of cyclobutane (i.e., dioxetane for the addition of O_2 and cyclobutanone for the addition of ketene) and the other completely different (i.e., peroxirane in one case and 2-methyleneoxetane in the other). The truly remarkable fact is that when the mode of ethylene addition is similar to that of the ethylene + ethylene cycloaddition, the topology of the potential energy surface is virtually identical.